ARTICLE

Check for updates

Microbial necromass carbon and nitrogen persistence are decoupled in agricultural grassland soils

Kate M. Buckeridge [1,2 ✉], Kelly E. Mason [3], Nick Ostle[2], Niall P. McNamara[3], Helen K. Grant[3] & Jeanette Whitaker [3]

Microbial necromass is an important component of soil organic matter, however its persistence and contribution to soil carbon sequestration are poorly quantified. Here, we investigate the interaction of necromass with soil minerals and compare its persistence to that of plant litter in grassland soils under low- and high-management intensity in northwest England. During a 1-year laboratory-based incubation, we find carbon mineralization rates are higher for plant leaf litter than root litter and necromass, but find no significant difference in carbon persistence after 1 year. During a field experiment, approximately two thirds of isotopically-labelled necromass carbon became mineral-associated within 3 days. Mineral-associated carbon declined more rapidly than nitrogen over 8 months, with the persistence of both enhanced under increased management intensity. We suggest that carbon mineralisation rates are decoupled from carbon persistence and that necromass carbon is less persistent than necromass nitrogen, with agricultural management intensity impacting carbon sequestration in grasslands.

[1] Luxembourg Institute of Science and Technology, Belvaux, Luxembourg. [2] Lancaster Environment Centre, University of Lancaster, Lancaster, UK. [3] UK Centre for Ecology & Hydrology, Lancaster, UK. ✉email: kate.buckeridge@list.lu

Soils store 1580 Pg (i.e. 10^{15} g) carbon (C)—more than the atmosphere (750 Pg C) and vegetation (610 Pg C) combined[1]—and contain a small but influential slice (460 Pg N) of the global nitrogen (N) pool (~2×10^{23} g N)[2]. Consequently, small changes in soil storage of C and N have ramifications for global biogeochemical cycles and food security[1,3]. Grasslands, representing 3360 Mha or 68% of global agricultural land[4], are particularly important as they contain large amounts of soil organic C (SOC; 343 Pg C in the top 1 m)[5]. This SOC stock is influenced by land use intensity, although the direction of change and mechanisms of loss or gain vary with different management practices[6].

Multiple analytical methods have revealed that soil microbial products and residues (hereafter 'microbial necromass' or 'necromass') either dominate or contribute substantially to persistent soil organic matter (SOM), especially in grasslands[7–15]. This research indicates that the formation of stable necromass C is influenced by multiple factors that influence live and dead microbes (i.e., spatial location, microbial density and taxa, abiotic conditions)[16], and also that stable necromass C formation (as with all stable SOM) is strongly influenced by soil mineralogy[17,18], and often begins with adsorption to mineral surfaces[19–22]. It is also evident that microbial metabolism influences the formation and loss of mineral-associated necromass C[23–25], but the importance of microbial necromass consumption by live microbes (i.e., necromass recycling)[26] and the persistence of necromass association with mineral surfaces are less clear. In this study we aim to address three key uncertainties: 1) if microbial substrate type (microbial necromass versus plant litter) impacts the formation of persistent soil C; 2) how much microbial necromass C and N are recycled versus associated with soil minerals; and 3) at what rate microbial necromass C and N associated with soil mineral surfaces are lost (Fig. 1a).

Soils contain a diverse array of microbial and plant-derived substrates which vary in their chemistry. This influences the microbial decomposition rate of these substrates and will potentially affect their persistence[27]. Soil microorganisms may decompose microbial necromass faster than plant litter because it has a lower C:N ratio, which is a consistent indicator of microbial substrate preference[28]. In contrast, soil microbes may decompose plant litter faster than microbial necromass because most heterotrophic microbes are C-limited[29], especially in N-rich agricultural grasslands. Soil microbes may also decompose plant litter faster than microbial necromass because necromass contains specific compounds that are resistant to decomposition[30]. A comparison of microbial decomposition of plant litter versus microbial necromass and the influence of decomposition rate on persistent SOM formation will clarify the importance of microbial substrate preference on microbial necromass persistence.

The formation, persistence and loss of microbial necromass C may change with the intensity of grassland management, of particular concern as the degradation of grasslands continues globally[5]. For instance, management alters plant and microbial community structure and microbial processing of C and N[31], all of which also influence C persistence[20]. If labile plant exudate and fertilizer N is rapidly immobilized by pasture grasses in high-intensity grasslands, microbial necromass N may be preferentially used by soil microbes[17]. Microbial necromass studies primarily focus on necromass C, yet necromass N may be particularly important for addressing our knowledge gaps[32], as microbial `necromass is N-rich compared to plant inputs. Because of its higher N content[12,33] microbial necromass may also have a stronger affinity for mineral surfaces than plant litter, for instance due to preferential sorption of proteins relative to polysaccharides[34]. There is evidence that sorption to clean mineral surfaces favours molecules rich in N[10]. Therefore, N

content could increase the likelihood of microbial necromass persistence and thus make it less accessible for loss by microbial decay. Understanding microbial recycling, stabilization and destabilization of microbial necromass N is not only critical for agricultural grassland management with strict N-accountability;[35] its influence on soil C sequestration may be a major gap in our understanding of the fate of microbial necromass.

Microbial necromass C and N association with mineral surfaces may be reduced by necromass recycling. We define recycling as microbial decomposition of dead microbes and microbial products, resulting in necromass C and N assimilation into biomass, or loss through mineralization[26] before mineral-association, distinct from necromass removal from mineral surfaces (destabilization or mining) (Fig. 1a)[16]. Soil microbes use microbial necromass as a growth substrate[26,36–38]. However, abiotic interactions that lead to necromass mineral-association can be immediate and substantial[17,39], and may be faster than microbial uptake of necromass for substrate. Once protected by mineral association, it has not been quantified how long necromass remains, or to what extent mineral-associated necromass may be mined by soil microorganisms. Microbial necromass destabilization via mining (i.e., biotic desorption, such as through the production of organic acids or proximate extracellular enzymes[40]) may be particularly important in diverse grasslands under low-intensity management, where plant communities have reduced winter photosynthate inputs and rhizosphere microbes are potentially C-limited[29]. In addition, precipitation, seasonal flooding, or macrofaunal bioturbation may increase necromass loss by stimulating aggregate turnover, and plant root exudates may promote loss by contributing organic acids and stimulating priming (i.e., mineralization of native SOM, including necromass)[41,42]. Furthermore, it is unclear what role necromass N plays in the role and timing of recycling or loss of necromass C. Using stable-isotopes to examine the fate of C and N independently and as a ratio can provide insight into controlling mechanisms such as microbial mining and turnover (Fig. 1b, c).

Here, a laboratory and field experiment were conducted to investigate the influence of microbial substrate mineralization on persistence, and the rate at which microbial necromass is sorbed and removed from soil minerals. In both experiments, a single addition of dual isotope-labelled ($^{13}C^{15}N$) substrate (necromass and plant root and leaf litter in the lab and necromass in the field) was added to soil and tracked over time. In the lab experiment, we detected higher microbial substrate mineralization rates for plant leaf litter over root litter or necromass, yet we saw no influence of these rate differences on C persistence after 1 year. This is in contrast to theory that substrate complexity is related to lower carbon use efficiency and lower mineral-associated C formation[20]. Our field experiment demonstrated that 64% (±5%) of the added, labelled necromass was recovered in the mineral-associated fraction within 3 days. A much smaller amount of the initial amount added was recovered in the microbial biomass (C: 2.1 ± 0.2%; N: 4.7 ± 0.7%) with the remainder being mineralized or leached. Over the course of the field incubation (238 d), half (53%) of this added necromass-C that became mineral-associated was subsequently lost through microbial mining, and 81% of the mineral-associated necromass N persisted. Our study demonstrates that (a) differences in microbial decomposition rates do not necessarily translate to differences in C persistence between plant litter and microbial necromass, and (b) microbial necromass C and N are rapidly sorbed to minerals yet C is less persistent than N, especially in high- versus low-intensity agricultural grasslands. This decoupling of C and N destabilization can be used to improve the next generation of ecosystem process models.
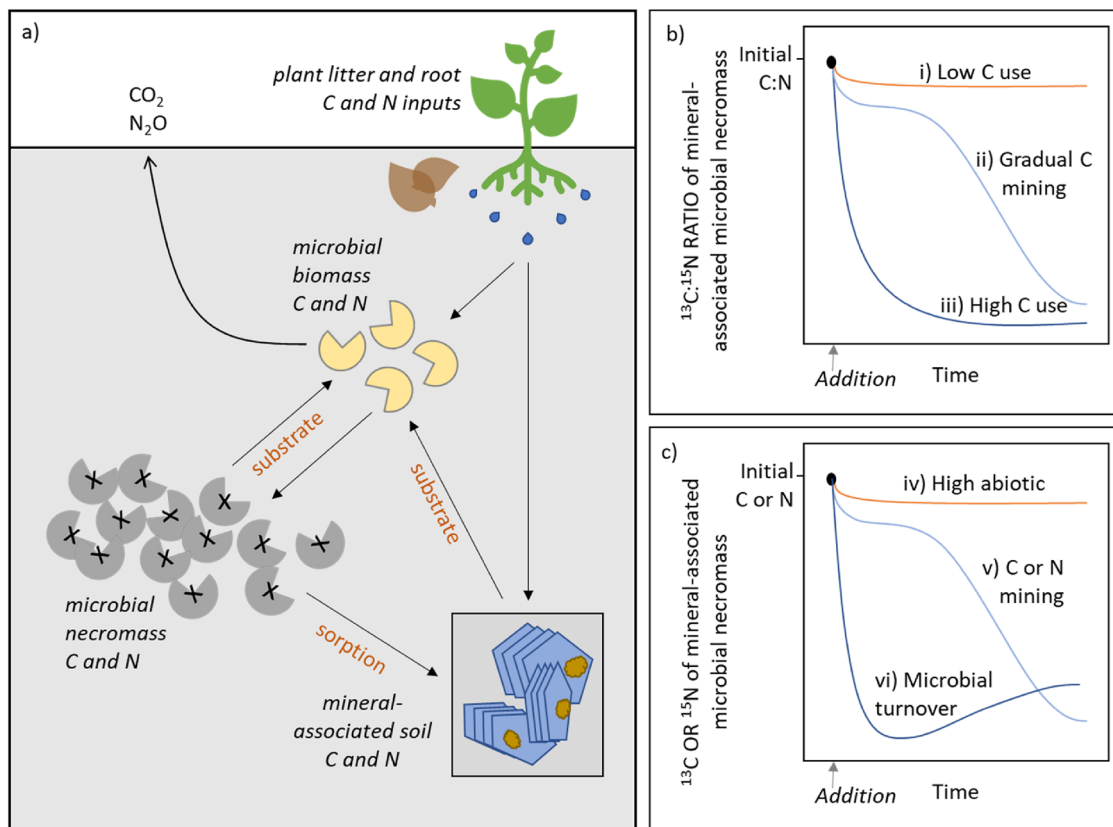
Fig. 1 The fate of microbial necromass in soil, and the hypothetical response curves for stable-isotope tracing of mineral-associated microbial necromass in soil as a tool to assess that fate. a A representation of how plant carbon inputs to soil may directly adsorb to fine minerals, or be consumed by microbial biomass then become necromass. Here we quantify how necromass may be recycled by microbial biomass as substrate, sorbed to fine minerals, and then mined from mineral surfaces by soil microbes. **b** We traced isotopically-labelled microbial necromass to sorption on fine minerals and used the $^{13}C{:}^{15}N$ ratio of the mineral-associated necromass to indicate sustained low use of necromass-C as microbial substrate and high sustained C mineral-association (i), or gradual microbial C-limitation and C-mining of mineral-associated necromass-C pools (ii), or rapid use of necromass-C as microbial substrate with no microbial mining (iii). **c** We assessed the ^{13}C or ^{15}N of the mineral-associated necromass to indicate if rapid abiotic interaction of necromass on fine minerals was high as hypothesized (iv) or initially low (vi), and if this initial state was followed by loss from microbial mining of C or N (v), versus gradual accumulation of necromass-C or N, for instance as a result of turnover of the biomass that consumed necromass C or N (vi).

Results and discussion

Decomposition and persistence of plant litter versus microbial necromass. Our first aim was to assess the influence of substrate type—plant litter or necromass—on decomposition rate and C and N persistence. Soils were sampled from juxtaposed, low- and high-intensity grasslands ($n = 5$; Supplementary Table 1). Presumably because of long-term (>35 y) differences in management, high-intensity grasslands had higher microbial biomass carbon (MBC), a more depleted soil $\delta^{13}C$ and a less depleted soil $\delta^{15}N$ natural abundance signal (Supplementary Table 1; $P < 0.05$). These grasslands also differed in microbial community structure (Supplementary Fig. 2), plant biomass (Supplementary Table 3) and plant community structure (Methods). The soils were amended with one of dual isotopically-labelled ($^{13}C^{15}N$) *Escherichia coli* (bacterial necromass), *Lolium perenne* (rye grass leaf or root litter), or no addition (soil only controls) in separate glass jars in a 1 year lab incubation. The added necromass was prepared by growing *E.coli* on $^{13}C^{15}N$ isotopically-enriched media, then autoclaving (2x), lyophilizing, and resuspending the mass; the *L. perenne* was grown from seed with daily $^{13}CO_2$ fumigation and weekly $K^{15}NO_3$ amendments (see Methods for details). A single species of necromass and of plant litter were used as a proxy for all necromass/plant litter, recognizing that a single species cannot represent the chemical complexity of the complete soil bacterial or plant community. The validity of this approach is

inconclusive: previous studies have demonstrated that necromass taxa do not influence decomposition rates of necromass[38], and that plant litter decomposition is strongly controlled by C:N (or C:P) which may or may not vary by species[43]. However, a growing number of studies reveal species effects for fungi on necromass decomposition due to variation in chemistry[44] or morphology[45]. Bacterial taxa may also influence necromass retention on mineral surfaces by interacting with fungal morphology or chemistry[39]. To resolve these contradictions, we anticipate that future studies may compare species effects on this comparison of plant versus microbial inputs in terms of forming mineral-associated C. Here, we hypothesized that decomposition rates would decline with substrate quality (following a gradient of low to high C:N ratio) and predicted the highest mineralization rate from necromass, followed by plant leaves, then roots[28]. We hypothesised that high quality (low C:N) substrates would induce greater necromass formation[20] and necromass-mineral association than low quality substrates due to the higher efficiency of microbial substrate use (i.e., favouring r-selected taxa with higher growth and death rate). We expected this difference to be amplified in grassland soils under historical high-intensity management due to the greater nutrient availability and a history of high-quality plant inputs to the rhizosphere.

Microbial decomposition was indicated by substrate-derived CO_2 and N_2O efflux, and both were generally higher from leaves
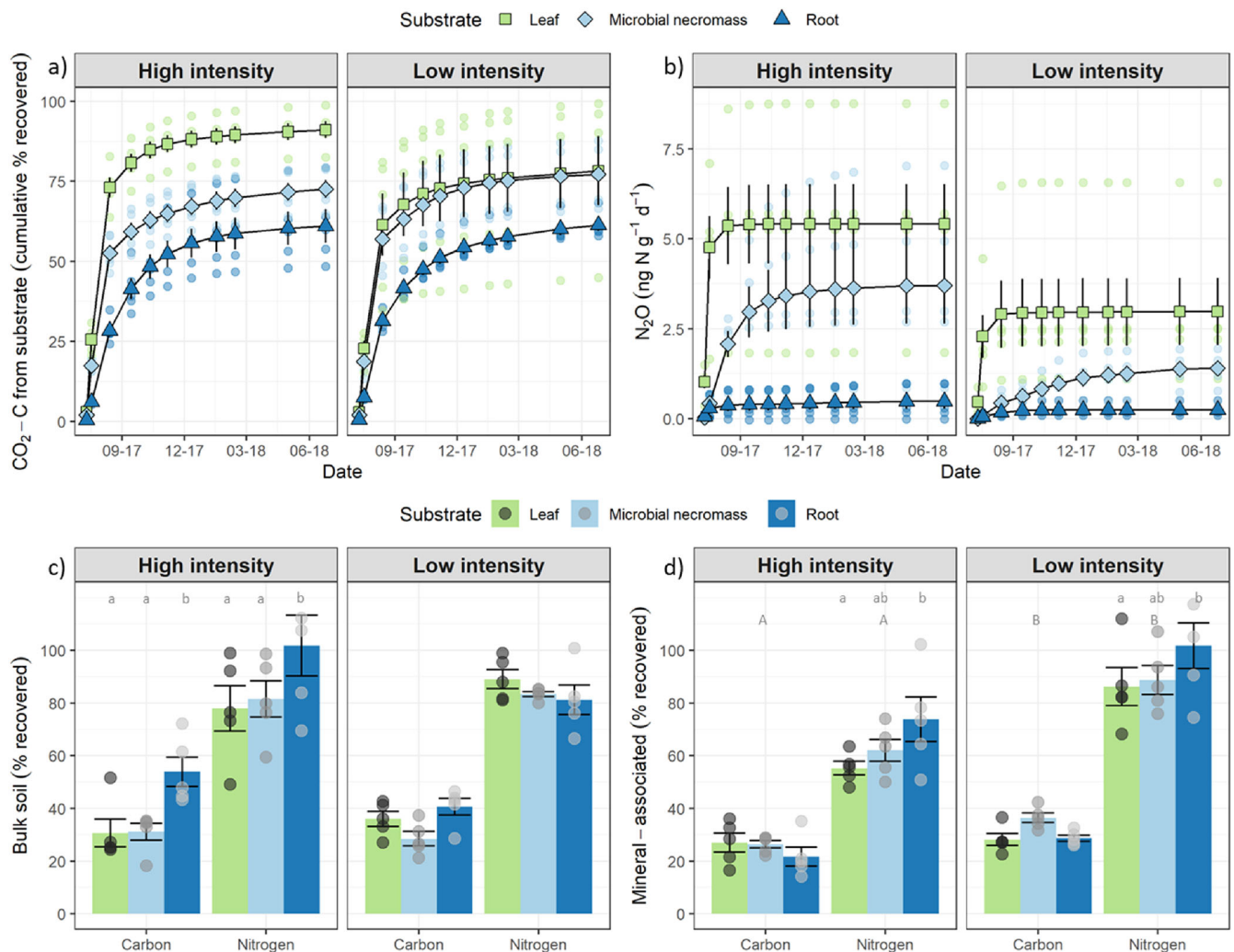
Fig. 2 Microbial substrate preference does not influence substrate C stabilization. The cumulative mean (and standard error, $n = 5$) % recovered of added $^{13}C^{15}N$-labelled *Lolium perenne* litter ("Leaf" & "Root") or *E. coli* necromass ("Microbial necromass") as CO_2-C (**a**), N_2O-N (**b**) and remaining in bulk soil (**c**) indicates differences in microbial substrate preference during a 1-year lab incubation, whereas the amount of fine (<53 μm) mineral-associated C and N (**d**) is a proxy for stable SOM, and does not reflect these microbial substrate preferences. Low land management intensity enhanced mineral-associated C and N, and roots (low microbial preference) increased the amount of mineral-associated N recovered, whereas C mineral-association was not influenced by microbial substrate preference. Small letters above bars in (**c**, **d**) indicate a significant difference between substrates (within element, across land uses), and capital letters indicate a significant difference between land uses (within element, across substrates). There were no significant interactions between substrate and land use for bulk and mineral-associated soil. A summary of statistical interactions for (**a**, **b**) is found in Supplementary Table 2.

than necromass, and from necromass more than roots (Fig. 2a, b), with some variation by land management (Supplementary Table 2). In this laboratory incubation, the substrate-derived C and N remaining in the bulk soil pool represent C and N that were not released as gaseous efflux. As expected, the patterns here were the reverse of substrate use such that in the bulk soil there was higher root C remaining as compared to necromass C ($P = 0.0008$) or leaf C ($P = 0.0085$, Fig. 2c). Also in contrast with gaseous efflux, the N signal in bulk soil did not differ between substrate types in a consistent manner across land management (Fig. 2c) and there was no land management effect or interaction for substrate C or N in bulk soil. These results—indicating a preference for leaves > necromass > roots—did not support our hypothesis or our underlying assumption that microbial use was driven by substrate quality, suggesting that the C:N ratio is not the dominant predictor of decomposition rates, at least between *L. perenne* and *E. coli*. The microbes in these incubations may have been C-limited in the absence of fresh plant exudate

inputs[29]. Furthermore, a select subset of the microbial community may be consuming necromass[26], supported by the treatment interactions between residue types and land management for both substrate-derived CO_2 and N_2O (Supplementary Table 2) and by differences in the microbial community composition between these two soils (Supplementary Fig. 2).

Our lab incubation compared the proportion of microbial and plant C and N added that was mineral-associated after 1-year by quantifying the mass of label in the fine mineral (<53 μm) pool. In contrast to our hypothesis and dominant theory of stable SOM-formation[20], we found no significant difference in accumulation of mineral-associated C between soils containing *E. coli* necromass and *L. perenne* leaf litter (Fig. 2d), although there was more mineral-associated N in soils containing roots as compared to leaves ($P = 0.032$). There was no interaction between management and residue type; however, low-intensity soils accumulated more mineral-associated C ($P = 0.0056$) and N ($P < 0.0001$) than high-intensity managed soils, complementing

the generally lower C and N efflux rates from these soils. These lab incubations therefore do not support the theory that lower complexity, rapidly cycling substrate is more likely to become mineral-associated C[20], at least over the course of the first year and in the absence of plants.

Microbial necromass fate and persistence. Our second and third aim, to investigate the fate and persistence of necromass in soil (Fig. 1b, c), were achieved by tracing isotopically-labelled ($^{13}C^{15}N$) *E. coli* necromass in a field experiment over the course of ~8 months (238 d) in the same juxtaposed grasslands sampled for the lab experiment (Supplementary Table 1). As with the lab assay, our investigation explored the historical effect of management intensity. We injected the necromass as a suspension (or water in the control plots) in 20 cm diameter collars (see Methods for details), replicated for four time points (allowing for destructive harvests), in 5 replicate blocks. Our method of necromass addition was intended to mimic the production and subsequent expulsion of necromass from soil biofilms that may be linked to biofilm dispersal (e.g.,[46]), which would introduce necromass into the wider soil environment. It is possible that mineral-associated necromass is dominated by mineral-associated microbes living and dying in situ—in this case, our method has quantified only a small portion of necromass fate. Resolving the importance of these two (or other) pathways of necromass production will require microscale spatial analysis of necromass production in future studies[16].

Pool sizes and isotopic signals of C and N in CO_2 and N_2O were measured in control and necromass subplots 1, 3, 21, 49, 92, 155 and 238 days after necromass addition. Pool sizes and isotopic signals of C and N in the microbial biomass, bulk SOM, and mineral-associated SOM were measured when soil in the collars was destructively sampled at 3, 21, 92, and 238 d after addition. The surface soil (Ap horizon) was sampled at two depths: 0–5 cm, which formed the pasture rhizosphere root-mat and enveloped the depth of necromass injection (1–3 cm); and 5–10 cm, which was below most of the pasture grass root biomass and the injection zone. The 10–20 cm depth was analysed after 238 d to assess any downward distribution of the injected necromass to the bottom of the Ap horizon (here we recovered 11.6% (±2.2%) of the added C, 20.4% (±3.4%) of the added N). Specifically, we wanted to know how much necromass C and N would be associated with fine soil minerals (<53 μm, assessed with physical fractionation; Supplementary Table 1 for bulk and mineral-associated pool sizes), and if association was due to a rapid initial sorption (i.e., abiotic) or a slowly-accumulating process (i.e., microbial uptake of necromass followed by turnover and release of N; leaching promoting release of organically bound necromass-N; or plant uptake of necromass-N followed by root exudation or root turnover and release of this N)(Fig. 1b, c). We then investigated whether mineral-associated C and N decreased over the course of the 238-d experiment, and if this decay in mineral-associated C and N pools was influenced by historic land management intensity. Based on short-term (3 d) laboratory studies[39], we hypothesized that most of the added necromass would be rapidly mineral-associated but then decline with time due to microbial mining (Fig. 1b, c). We also hypothesized that necromass persistence after 238 d would be higher in high-intensity managed grassland soils with higher plant root exudates and faster microbial turnover and necromass production.

Much of the added necromass was recycled and quickly mineralized as microbial substrate. Necromass-derived respiration ($^{13}CO_2$) was highest three days after necromass substrate addition (6.1 ± 0.6% of added necromass-C was respired on that day) before declining sharply (Fig. 3a), and there was no effect of land management intensity or interaction with time. In contrast, a very small proportion of added necromass-N was detected as $^{15}N_2O$, yet there was higher cumulative necromass-derived N_2O in the low-intensity (1.6 ± 0.8%) versus high-intensity (0.2 ± 0.06%) plots (P = 0.021; Fig. 3b). This management response was strongly influenced by one sampling date shortly after addition, which may have represented a hot moment, or a large, short-term pulse of N_2O, typical of the high spatial and temporal variation in soil N_2O efflux[47]. Higher N_2O efflux in the low-management plots was possibly a result of an interaction between necromass addition and historic higher plant litter inputs (Supplementary Table 3), and different plant and microbial communities (Methods, Supplementary Fig. 2), as N_2O hot spots and hot moments are known to be increased by plant residues[48].

We recovered 2.1 ± 0.2%, of the added necromass C and 4.7 ± 0.7% of the necromass N in the microbial biomass in the surface 10 cm of soil in the first 3 days after substrate addition. Most of the C and N recovered in the microbial biomass was in the 0–5 cm depth, with the amount differing between sample dates for microbial biomass C (P = 0.0004) and N (P = 0.0009), potentially due to necromass recycling into new microbial biomass with microbial turnover (Figs. 1c and 3c, d). However, the quantity of applied necromass C and N detected in the microbial biomass declined sharply over winter (92–238 d) indicating a seasonal microbial turnover[49] that would contribute to native (i.e., not injected) necromass production (Fig. 3c, d). Quantifying this type of seasonal production would require high frequency amino sugar analysis, or isotope dilution of amino sugars[50], which we did not perform in this study. Soil microbes in the 0–5 cm depth high-intensity plots, averaged across all time points, had higher concentrations of the added necromass C (P = 0.04) and N (P = 0.03) than in the low-intensity plots. However, microbial necromass C and N uptake by live soil microbes was unaffected by land management at the 5–10 cm depth. Averaged across all plots, 0.78 ± 0.08% of the added necromass C and 1.42 ± 0.15% of the added necromass N remained in the 0–20 cm microbial biomass at the end of our experiment, representing ~0.001% of the microbial biomass C and ~0.006% of the biomass N (Supplementary Fig. 3c, d). These results support two possible mechanisms: either that soil microbes will use only a small proportion of necromass for anabolism, or, that only a select segment of the microbial community (the necrobiome) will grow efficiently on necromass substrate[16,26]. In general, microbes prefer new versus old SOM and their carbon use efficiency (growth to respiration ratio) is lower on old SOM[51]. Therefore, future studies should examine whether added necromass has a low microbial uptake due to qualities unique to necromass that attract a necrobiome, or as a result of a general preference for new SOM.

Most of the added necromass became mineral-associated SOM within 3 days, consistent with results from short-term lab incubations[17,39]. A large amount of the added necromass C (64.1 ± 4.6%) and N (108.9 ± 5.7%) was mineral-associated in the top 10 cm of soil, three days after addition (Fig. 4a, b). Surprisingly for north-west England, there were no rain events during this initial period of the experiment. As a result, the soils were mesic (0.64 ± 0.01 g H2O g⁻¹ dw soil for 0–10 cm), which meant that soil moisture probably did not limit microbial activity nor promote leaching. The distribution of necromass C and N differed with land management intensity, with more mineral-associated necromass in the upper 0–5 cm (C: P = 0.029, N: P = 0.00022) in the high-intensity grassland and more mineral-associated necromass at 5–10 cm depth (C: P < 0.0001, N: P < 0.0001) in the low-intensity grassland. However, averaged across 0–10 cm depth, land management intensity had no effect
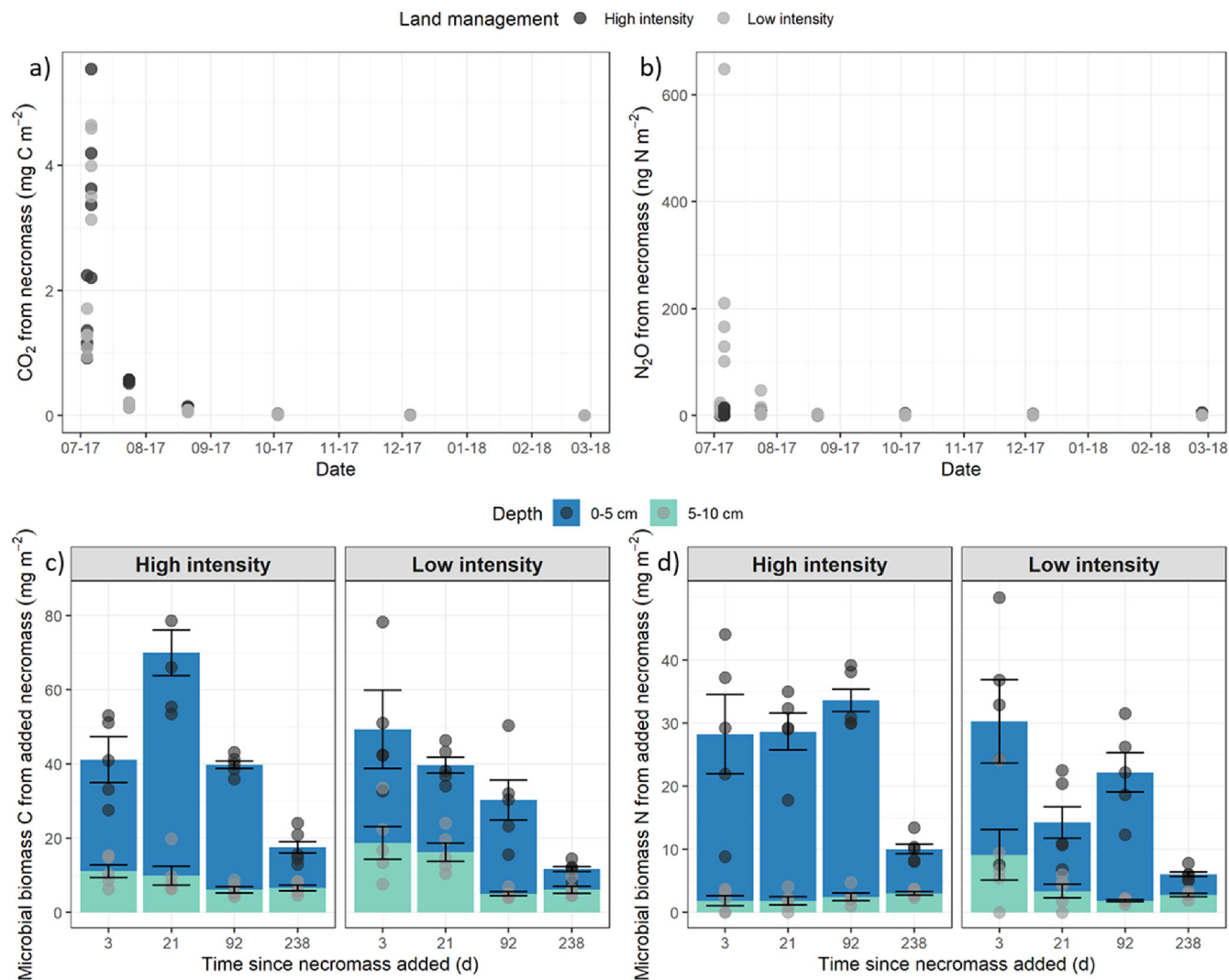
Fig. 3 Less than half of the field-added necromass carbon was mineralised or consumed by microbes. Mean (and standard error, n = 5) carbon and nitrogen from the added necromass released as CO_2-C (**a**), and N_2O-N (**b**), and recovered in the microbial biomass C (**c**), and the microbial biomass N (**d**), in high- and low-intensity pastures soils at two soil depths (0–5 and 5–10 cm). $^{13}C^{15}N$-labelled *E. coli* necromass (2.14 g C and 0.62 g N m^{-2}) was injected on 3/07/17, 1 day before the first gas sample point.

on the amount of necromass C and N that was mineral-associated. These results contrast with what we found in the lab, where there was higher mineral-association in low-intensity managed soils. This contrast between in situ results and plant-free lab incubations (with shared soil type but contrasting plant communities between treatments) suggests that the plant community and rhizosphere microbes play a critical role in net C persistence[52], both through producing photosynthate that fuels microbial growth and necromass production, and by releasing organic acids that destabilize C from mineral surfaces. Similarly, the different plant communities may have contributed to the strong depth differences between mineral-associated necromass C between land-use treatments (Fig. 4a, b). The relatively dense, short roots (and higher proportion of rhizosphere to bulk soil) in the high-intensity pasture grasses may have retained the injected necromass near the surface whereas the deeper-rooting forbs and tall-stem grasses in the low-intensity pasture may provide preferential flow paths[53] for water, nutrients, and our injected necromass to the 5–10 cm soil depth. Finally, the lack of plant N uptake in the lab incubations probably influenced microbial access to necromass N and may have elevated N_2O efflux, as indicated by the lower N_2O losses in the field experiment

(Fig. 3b). Alternatively, the lower N_2O losses in the field may be due to other factors, such as a higher N_2:N_2O efflux ratio, higher NO_3^- leaching, uncaptured spatial variability, or stronger fluctuations in O_2, as these factors also contribute to N_2O emissions[54].

Our third aim was to investigate the rate of loss of necromass from mineral surfaces. Our results indicate necromass C and N decay from mineral surfaces, with a faster decay rate for C (Fig. 4a–d). This disproportionate loss of C versus N suggests that microbial mining of C—possibly combined with stronger binding of proteins—was the main process controlling this loss (Fig. 1b, c). The C:N of the mineral-associated necromass in all plots and depths declined from 3.2 when added, to 2 on day 3, and 1.2 on day 238 (Fig. 4c). This declining C:N ratio also supports the concept of microbial mining for C and is consistent with the view that necromass N has a slower turnover time than necromass C[7].

To estimate the mean residence time of necromass C and N in this experiment and to compare our results to other studies, we fit linear models to the log-transformed variables and assumed that the slopes represented the pool turnover times. Necromass loss was indicated by the negative slope of the mineral-associated necromass C and N pools and differed with land management
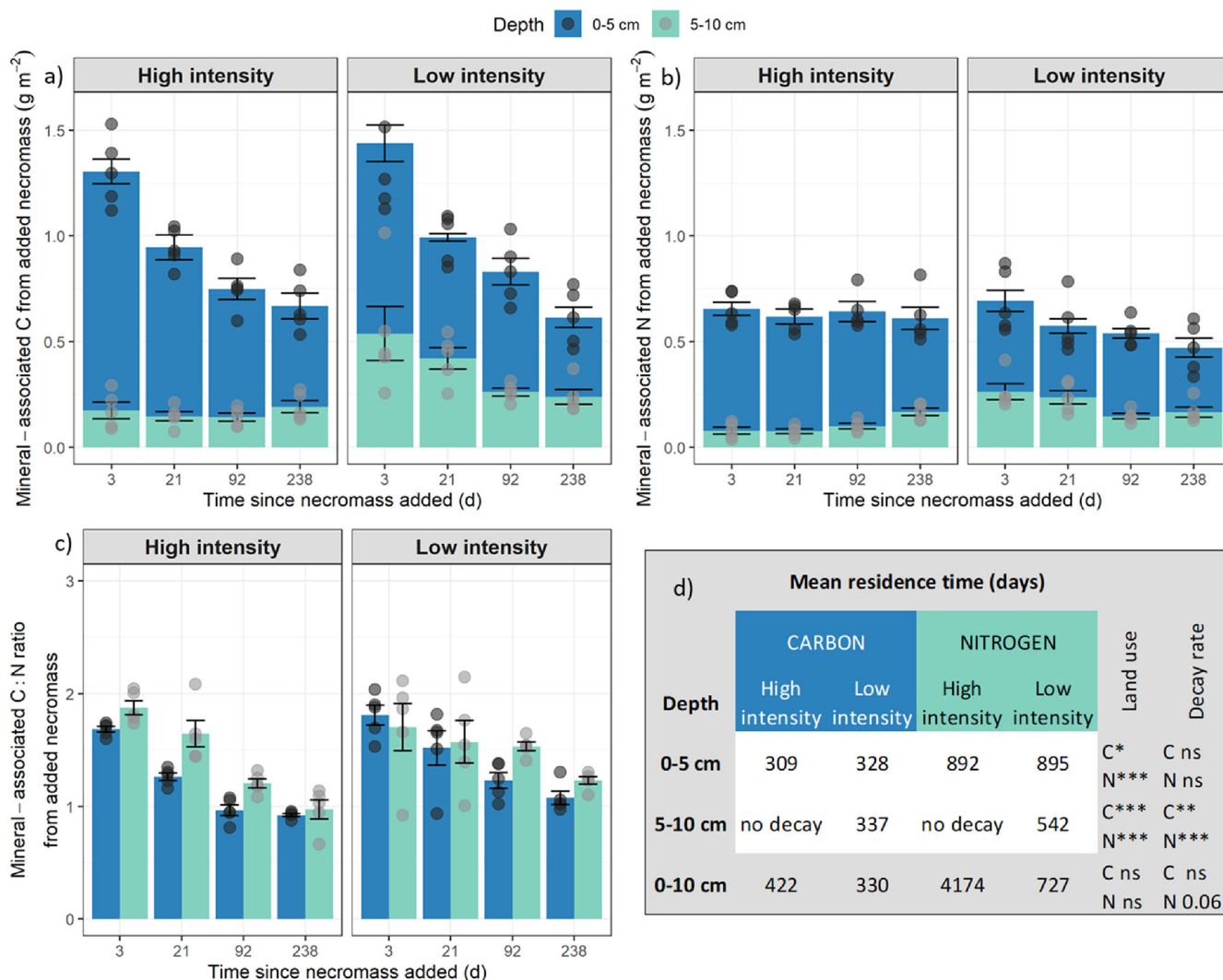
Fig. 4 Injected ^{13}C^{15}N-labelled *E. coli* necromass rapidly becomes mineral-associated soil organic matter, then necromass carbon is mined faster than nitrogen. Mean (and standard error, $n = 5$) necromass-derived carbon (**a**), nitrogen (**b**) and carbon:nitrogen ratio (**c**) associated with fine minerals (<53 μm particle size), as quantified by elemental and isotopic analysis following physical fractionation, in high- and low-intensity pastures soils at two soil depths (0–5 and 5–10 cm) over 238 d. (**d**) The mean residence time of the added necromass carbon and nitrogen was calculated from the inverse of the slope of the decay rate (ln(pool) ~ time) for the two depths (0–5 & 5–10 cm) and the depth total (0–10 cm). Significance codes for differences between land use (intercept) and land use decay rate (slope): $^{***}P < 0.001$, $^{**}P < 0.01$, $^{*}P < 0.05$, ns not significant.

intensity only in the 5–10 cm soils (C: $P = 0.0036$, N: $P < 0.0001$), because there was no detectable loss at this soil depth in the high-intensity treatment (Fig. 4d). This conflicts with our hypothesis that necromass would be more persistent in the high-intensity soils driven by higher necromass production and turnover. Instead, these high-intensity 5–10 cm soils appear to have a reduced loss rate of mineral-associated SOM. Therefore, both gains (rapid mineral-association) and losses (destabilization) of C and N (Fig. 4a, b) were reduced in the high-intensity plots at 5–10 cm depth, as compared to the low-intensity plots dominated by deeper-rooting tall stem grasses and forbs (see Methods for plant community descriptions). Necromass N may be accumulating in N-rich high-intensity soils below the plant rooting zone in part because of slow microbial consumption due to microbial N saturation. Our results also tentatively support the concept that N-replete soils may display negative priming[55], and that plant exudate priming[56] may facilitate microbial mining of necromass.

The inverse of turnover represents a simple estimate of the mean residence time of added necromass C and N, assuming a homogenous quantity of material entering the soil at a single time point before departing—real chemical complexity of microbial necromass with multiple pools will provide a better estimate for future studies, especially if recycling between pools is considered[57,58]. Nonetheless, our exponential decay model implies that averaged across the 0–10 cm depth, necromass C was retained for 330–422 d (Fig. 4d) in these grassland soils, and necromass N was retained for 727–4211 d, with a trend for longer retention in soils with high-intensity management ($P = 0.060$). These in situ C residency times are ~2x longer than estimates derived from ^{13}C-labelled substrate tracing;[59] the ^{15}N-labelled necromass estimates are comparable to other studies[60]. At 238 d after injection, averaged across all plots, $37.1 \pm 1.9\%$ of the added necromass C and $105.2 \pm 6.3\%$ of the added necromass N remained in the 0–20 cm mineral-associated pool.

Implications for soil organic matter persistence. There is strong evidence that necromass is a major component of SOM but we are only just beginning to understand the dynamic interactions that govern its mineral sorption and persistence. Our findings illustrate that multiple, interacting processes are operating in soil

with necromass being transformed through a continuum of stages, including production, recycling, stabilization and destabilization[16]. Although all SOM progresses through transformation stages in soil, the chemical and morphological characteristics of microbial necromass, as well as the activity and composition of the soil microbial community, probably influence the rates and timing of these stages. Microbial substrate mineralization rates did not result in differences for mineral-associated C in our lab incubations despite theory that substrate complexity is associated with lower substrate use efficiency and mineral association. The different land management effects in our lab and field assays—with more C persisting in the lab in low-intensity soils and less C persisting in the low-intensity rhizosphere soils in the field—suggest that differences in plant and rhizosphere communities due to management have a large impact on the dynamics of accumulation and loss of mineral-associated necromass, and therefore on potential C sequestration rates. Furthermore, in our study, despite 8 months in field conditions and evidence of microbial mining of mineral-associated necromass, 53% of the added necromass C and 81% of necromass N were still present in the upper 10 cm of soil. This demonstrates a decoupling of C and N persistence, which is a potential mechanism for the accumulation of N in agricultural grasslands and supports further studies to minimize C mining through changes to agricultural management. Insight into the necromass continuum in soil presents new opportunities for climate change mitigation, via manipulation of the different stages (Fig. 1a). It also provides insight into the timing of C and N decoupling; information that could be used to improve the next generation of ecosystem process models that more explicitly represent the soil mineral matrix in SOM formation and persistence[61].

Methods

Study site. This study was conducted in a clay loam agricultural soil (Chromic Eutric Albic Stagnosol, sand: 53%, silt: 19%, clay: 28%, pH: 6.7) in an over-the-fence pairing of high and low-intensity managed pastures at Myerscough College Experimental Farm in northwest England (53°50'57″N, 2°47'01″W, 10 masl). The Myerscough climate station reports a mean annual (1981–2010) maximum temperature of 14 °C, minimum temperature of 6 °C, and 1034 mm of precipitation. The high-intensity pasture (%C: 4.8, %N: 0.48) had a historic (10-year average) management of 247 kg N ha^{-1} y^{-1} (slurry and manure), 2–3 mows y^{-1} and 0.21 livestock units ha^{-1} y^{-1} (cattle equivalent). The plant community in 2017 were mostly grasses, dominated by: *Lolium perenne* (32%), *Poa trivialis* (30%) and *Stellaria media* (18%), with 5% or less of *Agrostis stolonifera*, *Poa annua*, *Rumex obstustifolia*, *Tripleurospermum inodorum*, *Alopecurus geniculatus*, and *Phleum pratense*. The low-intensity pasture (%C: 6.7, %N: 0.63) was unamended for the past 35 years, with very rare grazing. The low-intensity plant community in 2017 was a mix of tall-grasses and forbs, dominated by *Phalarus arundinacea* (19%), *Urtica dioica* (17%), *Elymus repens* (15%), *Convulvulus arvensis* (9%), *Cirsium arvense* (6%), and 5% or less of *Lathrys pratensis*, *Galium aperine*, *Alopecurus pratensis*, *Vicia sepium*, *Galeopsis tetra*, *Heracleum sphondylium*, and *Stachys sylvatica*. The high intensity pasture had higher plant biomass and lower litter biomass as compared to the low intensity pasture, during the sample period (Supplementary). The two pastures were separated by a drainage ditch and fence and in each field, 2 m^2 plots ($n = 5$) were established along a 100 m transect (20 m centre-to-centre), parallel to the fence at least 30 m from the ditch. Each plot was an experimental block containing 4 subplots (each 0.5 m^2). In the centre of each subplot, a PVC collar (20 cm diameter, 20 cm in height) was inserted into the ground to 10 cm depth. Land use intensity is a historical designation as all plots were removed from management in the year this experiment was conducted. Microbial community bacterial (16 S rRNA) and fungal (ITS) structure was ascertained from publicly-available data[26], for samples collected one year before this study, from the same fields, 0–15 cm depth. Microbial beta-diversity was compared between land use treatments using an Analysis of Similarity (anosim) test and a PCoA visualization of the Bray-Curtis distance matrices, within the vegan package in R[62].

Laboratory incubation with plant litter and microbial necromass additions. To estimate the relative stabilization of microbial versus plant residues, we carried out a one-year soil incubation with stable isotope-labelled residues added to the low and high-intensity pasture soils. Three soil cores (10 cm depth) were collected and composited from each plot ($n = 5$) and sieved to 2 mm. Fresh soil samples were moistened to 60% water-holding capacity and weighed (140 g oven-dry-equivalent)

into 1 L canning jars with air-tight lids containing septa for headspace gas sampling. As tracers, we used ^{13}C- and ^{15}N-labelled senesced *Lolium perenne* leaf (1.9547 atm% C, 1.1070 atm% N) and root (1.9077 atm% C, 0.7591 atm% N) and *Escherichia coli* necromass (1.9608 atm% C, 1.3398 atm% N). The *L. perenne* litter was grown from seed with daily pulses of 99 atm% CO_2 to a closed chamber, and weekly watering with 10 atm% K^{15}NO$_3$-amended Hoagland's solution, for 10 weeks, then water was withheld, and leaves and roots were harvested from the senesced plants, dried, and ground. The microbial necromass was started as frozen *E. coli* stock (NCIMB 12210), grown on streak plates, then as pure cultures established in a minimal M9 salts media base (($64 g$ Na$_2$HPO$_4$.7H$_2$O + 15 g KH$_2$PO$_4$ + 2.5 g NaCl) L^{-1}) augmented with 2 atm% ^{13}C-glucose (4 g L^{-1}) and ^{15}NH$_4$Cl (1 g L^{-1}). Cultures were grown in 2 L batches for 48 h at 37 °C in a rotary incubator shaker, spun down to a pellet (4600 x g), autoclaved twice, freeze-dried, then batches were mixed and ground to a powder.

The plant leaf and root litter and microbial necromass were added to the soil to create three treatments (plus a no-addition control) with equal amounts of necromass C (5.34 mg C g^{-1}) but unequal amounts of necromass N (leaf: 0.47, root: 0.14, microbial: 1.55, mg N g^{-1}). We incubated soils in the dark at 15 °C for 349 d and collected headspace gas over 24 h, after flushing the headspace, on day 1, 7, 34, 65, 93, 118, 153, 189, 217, 294, and 349. The jars had airtight lids for each 24 h gas sampling period, and between gas sampling periods, lids with a 1 cm-diameter hole to allow gas exchange and minimal moisture loss. Moisture loss was corrected by weekly water additions based on mass difference. At the end of the incubation, we performed physical fractionation in the same manner as above. C and N concentrations and isotopic values in the headspace gas and soil fine fraction were measured as above and used to assess microbial loss and biological stability of the three substrates.

Field experiment with dual-labelled microbial necromass tracing. To trace necromass C and N to soil microbial biomass and stable pools, lab-grown, isotopically-labelled *E. coli* necromass was added as a single pulse and tracked through time. The *E. coli* necromass was prepared as for the lab experiment, but with a modified amount of labelled ^{13}C-glucose and ^{15}NH$_4$Cl to obtain 99 atm% C and N. Just prior to application, the necromass was suspended in sterile ultra-pure water.

On 3 July 2017, necromass suspension was injected with a sideport needle in a 10-point grid pattern into the surface 3 cm of soil, inside PVC collars, as 140 mg of dry weight equivalent necromass per collar, or 2139.04 mg C m^{-2} and 619.25 mg N m^{-2}. The 20 cm diameter PVC collars were inserted into intact soil and vegetation (10 cm above ground, 10 cm below ground) two months before the start of the experiment. The experimental design consisted of a land-use treatment: high-intensity and low-intensity pasture, and a necromass treatment: with or without necromass (controls had water only injections), and time: a collar associated with each soil harvest that occurred on 6 July 2017 (3 days), 24 July 2017 (21 days), 3 October 2017 (92 days) and 26 February 2018 (238 days). The paired treatment (necromass) and control (water only) subplots in each block ($n = 5$) in an alternating pattern.

To estimate net gaseous flux of necromass C and N, flat, opaque chamber lids fit with septa were attached to the 8-month (final date) collars periodically (4 July, 6 July, 24 July, 21 August, 3 October, 5 December, 26 February), to create a chamber volume of 0.01 m^3, and headspace gas samples were collected over 30 min. Gas samples were analyzed for CO_2 and N_2O on a Perkin-Elmer Autosystem XL gas chromatograph (GC) fit with a methanizer and flame ionization detector (CO_2) and an electron-capture detector (N_2O). Headspace isotopic $^{12+13}CO_2$ and $^{14+15}N_2O$ were measured on Picarro G2131-*i* (CO_2) and G5131-*i* (N_2O) CRDS isotopic analyzers, calibrated against certified and internal standards with a precision of 0.5‰ standard deviation.

On each harvest date, the soil in one control and necromass collar in each block (across the two land-use treatments, i.e., a paired subplot) was destructively harvested from 0–5 cm and 5–10 cm depth and on the 26 February (time final sample), also from 10–20 cm depth. Soils were stored in plastic bags at 4 °C until processing, within two weeks of collection. Soils were sieved to 4 mm, then subsampled into two aliquots: (1) fresh soil for estimating necromass mobilization into microbial biomass, or (2) air dried soil for estimating necromass stabilization as mineral-associated organic matter.

Microbial biomass was extracted from two subsamples of fresh soil using a modified chloroform-direct extraction[63], with a water matrix (+ 1 ml CHCl$_3$ in one of the tubes) and reduced shaking time (2 h). Extractable organic C (EOC) and extractable nitrogen (EN) of the chloroform extracts and water extract controls were used to calculate the microbial biomass flush, on a Shimadzu TOC-L CPN (Shimadzu UK Ltd., UK). To measure necromass uptake into biomass, chloroform and control water extracts were freeze-dried, ground and analyzed for δ^{13}C on a Costech CN streamed to a Picarro G2131-*i* CRDS[64], and for δ^{15}N on a Carlo Erba NA1500 elemental analyzer coupled to a Dennis Leigh Technologies IRMS.

Mineral-association of the added necromass was assessed by measuring ^{13}C and ^{15}N accumulation on the soil fine fraction (<53 μm) in a method modified from Lopez-Sangil et al[65]. Specifically, air-dried soil (~5 g) was weighed into a 125 ml bottle with 5 glass marbles and 40 ml ultra-pure H$_2$O and shaken (150 rpm, 1 hr) to disrupt macro-aggregates. The slurry was sieved (200 μm) to remove the coarse sand, then sonicated (440 J cm^{-3}) to disperse micro-aggregates, and immediately

sieved (53 μm) to remove the fine sand. The remaining silt and clay fraction ('fine minerals', 'mineral-associated') was dried (65 °C), weighed and analyzed for C and N content, on a LECO Truspec elemental analyzer, and for $\delta^{13}C$ and $\delta^{15}N$, as above for the biomass.

Data analysis. For both the lab and field experiment, to determine amounts of necromass-derived C and N in the soil fine fraction, bulk soil, microbial biomass, and headspace gas, we converted $\delta^{13}C$ and $\delta^{15}N$ to atm%, then calculated the percent of each pool that was substrate-derived using an isotope mixing model:

$$\%CorN_{sub} = \frac{atm\%_C - atm\%_T}{atm\%_C - atm\%_S} * 100, \quad (1)$$

where $atm\%_C$ is the atm% ^{13}C or ^{15}N value of the C or N pool (CO_2-C, N_2O, MBC, MBN, soil fine or bulk C or N) from the control (water only), $atm\%_T$ is the atm% ^{13}C or ^{15}N value of the equivalent C or N pool from the substrate-added soils and $atm\%_S$ is the atm% ^{13}C or ^{15}N value of the labelled substrate. This $\%C_{sub}$ or $\%N_{sub}$ value was multiplied by the mass of the C or N pool from the 24 h incubation to calculate the absolute value of the substrate-derived C or N. Cumulative CO_2-C and N_2O-N from substrate was calculated using linear interpolation between sample points.

For MBC (and similarly for MBN), the calculation for percentage of substrate incorporation into microbial biomass flush was initialized by:

$$MBatm\%^{13}C = \frac{MBatm\%^{13}C_{fum} * C_{fum} - MBatm\%^{13}C_{unfum} * C_{unfum}}{C_{fum} - C_{unfum}}, \quad (2)$$

where MB atm% $^{13}C_{fum}$ is the atm% ^{13}C value of the microbial biomass from the $CHCl_3$-fumigated soil-water extract, C_{fum} is the C pool size of the $CHCl_3$-amended soil-water extract (μg C g^{-1} soil), MB atm% $^{13}C_{unfum}$ is the atm% ^{13}C value of the unamended soil-water extract, and C_{unfum} is the C pool size of the unamended soil-water extract (μg C g^{-1} soil). The control and treatment values for MB atm% ^{13}C were then incorporated into Eq. 1 to calculate the percentage of substrate incorporation into the microbial biomass ($\%MB^{13}C_{sub}$), then multiplied by the microbial biomass pool size (μg MBC g^{-1} soil) to convert to mass of substrate incorporated into the biomass ("$MB^{13}C$").

To investigate the effect of microbial substrate preference and land use on C and N bulk soil pools, mineral-association pools, and gaseous emissions, we used a two-way analysis of variance (ANOVA). To understand land use effects and temporal trends in necromass C and N soil stabilisation in the field experiment, we used a linear mixed effect model with land use and time since necromass addition as fixed effects and a plot x time interaction as a random effect to account for variation in the slopes with respect to time due to plot-specific differences. An autoregressive (AR1) correlation structure was added to the model to account for temporal autocorrelation between plots. We ran this model separately for each soil depth because: (a) our data did not have the power to include an additional factor in the model, (b) accumulation patterns clearly differed between the rooting depth (0–5 cm) and below (>5 cm), and (c) the magnitude of this difference between depths (partially an artefact of where the necromass was added (0–3 cm depth)) was less ecologically relevant than the pattern and controls. To estimate the mean residence time of the necromass C and N on the fine soil minerals and in the microbial biomass, we fit linear models with the log-transformed variables, assumed the model slopes represented the exponential decay functions (pool turnover time), and used their inverse for mean residence times. All models were fitted using the base, stats (version 3.6.3) and nlme[66] packages, and graphics were produced with ggplot2[67] (version 3.3.0) in R[62]. Data are publicly available[68].

Data availability

References

1. Intergovernmental Panel on Climate Change. Carbon and Other Biogeochemical Cycles. in *Climate Change 2013 – The Physical Science Basis: Working Group I Contribution to the Fifth Assessment Report of the Intergovernmental Panel on Climate Change* 465–570 (Cambridge University Press, 2014). https://doi.org/10.1017/CBO9781107415324.015.
2. Gruber, N. & Galloway, J. N. An Earth-system perspective of the global nitrogen cycle. *Nature* **451**, 293–296 (2008).
3. Houlton, B. Z. et al. A World of Cobenefits: Solving the global nitrogen challenge. *Earth's Futur.* **7**, 865–872 (2019).
4. Leifeld, J. et al. Turnover of grassland roots in mountain ecosystems revealed by their radiocarbon signature: Role of temperature and management. *PLoS One* **10**, 1–13 (2015).
5. Conant, R. T., Cerri, C. E. P., Osborne, B. B. & Paustian, K. Grassland management impacts on soil carbon stocks: A new synthesis. *Ecol. Appl.* **27**, 662–668 (2017).
6. Poeplau, C. Grassland soil organic carbon stocks along management intensity and warming gradients. *Grass Forage Sci.* **76**, 186–195 (2021).
7. Simpson, A. J., Simpson, M. J., Smith, E. & Kelleher, B. P. Microbially derived inputs to soil organic matter: Are current estimates too low? *Environ. Sci. Technol.* **41**, 8070–8076 (2007).
8. Grandy, A. S. & Neff, J. C. Molecular C dynamics downstream: The biochemical decomposition sequence and its impact on soil organic matter structure and function. *Sci. Total Environ.* **404**, 297–307 (2008).
9. Liang, C., Cheng, G., Wixon, D. L. & Balser, T. C. An Absorbing Markov Chain approach to understanding the microbial role in soil carbon stabilization. *Biogeochemistry* **106**, 303–309 (2011).
10. Miltner, A., Bombach, P., Schmidt-Brucken, B. & Kastner, M. SOM genesis: Microbial biomass as a significant source. *Biogeochemistry* **111**, 41–55 (2012).
11. Solomon, D. et al. Micro- and nano-environments of carbon sequestration: Multi-element STXM – NEXAFS spectromicroscopy assessment of microbial carbon and mineral associations. *Chem. Geol.* **329**, 53–73 (2012).
12. Kopittke, P. M. et al. Nitrogen-rich microbial products provide new organo-mineral associations for the stabilization of soil organic matter. *Glob. Chang. Biol.* **12**, 3218–3221 (2017).
13. Hall, S. J., Ye, C., Weintraub, S. R. & Hockaday, W. C. Molecular trade-offs in soil organic carbon composition at continental scale. *Nat. Geosci.* **13**, 687–692 (2020).
14. Angst, G., Mueller, K. E., Nierop, K. G. J. & Simpson, M. J. Plant- or microbial-derived? A review on the molecular composition of stabilized soil organic matter. *Soil Biol. Biochem.* **156**, 108189 (2021).
15. Kiem, R. & Kögel-Knabner, I. Contribution of lignin and polysaccharides to the refractory carbon pool in C-depleted arable soils. *Soil Biol. Biochem.* **35**, 101–118 (2003).
16. Buckeridge, K. M., Creamer, C. & Whitaker, J. Deconstructing the microbial necromass continuum to inform soil carbon sequestration. *Funct. Ecol.* (2022) https://doi.org/10.1111/1365-2435.14014.
17. Creamer, C. A. et al. Mineralogy dictates the initial mechanism of microbial necromass association. *Geochim. Cosmochim. Acta* **260**, 161–176 (2019).
18. Newcomb, C. J., Qafoku, N. P., Grate, J. W., Bailey, V. L. & De Yoreo, J. J. Developing a molecular picture of soil organic matter-mineral interactions by quantifying organo-mineral binding. *Nat. Commun.* **8**, 396 (2017).
19. Lehmann, J. & Kleber, M. The contentious nature of soil organic matter. *Nature* **528**, 60–68 (2015).
20. Cotrufo, M. F., Wallenstein, M. D., Boot, C. M., Denef, K. & Paul, E. The Microbial Efficiency-Matrix Stabilization (MEMS) framework integrates plant litter decomposition with soil organic matter stabilization: Do labile plant inputs form stable soil organic matter? *Glob. Chang. Biol.* **19**, 988–995 (2013).
21. Kaiser, K. & Guggenberger, G. The role of DOM sorption to mineral surfaces in the preservation of organic matter in soils. **31**, 711–725 (2000).
22. Kleber, M., Sollins, P. & Sutton, R. A conceptual model of organo-mineral interactions in soils: Self-assembly of organic molecular fragments into zonal structures on mineral surfaces. *Biogeochemistry* **85**, 9–24 (2007).
23. Bradford, M. A., Keiser, A. D., Davies, C. A., Mersmann, C. A. & Strickland, M. S. Empirical evidence that soil carbon formation from plant inputs is positively related to microbial growth. *Biogeochemistry* **113**, 271–281 (2013).
24. Liang, C., Amelung, W., Lehmann, J. & Kästner, M. Quantitative assessment of microbial necromass contribution to soil organic matter. *Glob. Chang. Biol.* **25**, 3578–3590 (2019).
25. Bailey, V. L., Pries, C. H. & Lajtha, K. What do we know about soil carbon destabilization? *Environ. Res. Lett.* **14**, 083004 (2019).
26. Buckeridge, K. M. et al. Environmental and microbial controls on microbial necromass recycling, an important precursor for soil carbon stabilization. *Commun. Earth Environ.* **1**, 1–9 (2020).
27. Wieder, W. R., Grandy, A. S., Kallenbach, C. M. & Bonan, G. B. Integrating microbial physiology and physio-chemical principles in soils with the MIcrobial-MIneral Carbon Stabilization (MIMICS) model. *Biogeosciences* **11**, 3899–3917 (2014).
28. Parton, W. et al. Global-scale similarities in nitrogen release patterns during long-term decomposition. *Science.* **315**, 361–364 (2007).
29. Soong, J. L. et al. Microbial carbon limitation: The need for integrating microorganisms into our understanding of ecosystem carbon cycling. *Glob. Chang. Biol.* **26**, 1953–1961 (2020).
30. Fernandez, C. W. & Koide, R. T. Initial melanin and nitrogen concentrations control the decomposition of ectomycorrhizal fungal litter. *Soil Biol. Biochem.* **77**, 150–157 (2014).
31. Malik, A. A. et al. Land use driven change in soil pH affects microbial carbon cycling processes. *Nat. Commun.* **9**, 3591 (2018).

32. Wang, X. et al. Elevated temperature increases the accumulation of microbial necromass nitrogen in soil via increasing microbial turnover. *Glob. Chang. Biol.* **26**, 5277–5289 (2020).

33. Possinger, A. R. et al. Organo–organic and organo–mineral interfaces in soil at the nanometer scale. *Nat. Commun.* **11**, 1–11 (2020).

34. Omoike, A. & Chorover, J. Adsorption to goethite of extracellular polymeric substances from Bacillus subtilis. *Geochim. Cosmochim. Acta* **70**, 827–838 (2006).

35. Van Meter, K. J., Basu, N. B., Veenstra, J. J. & Burras, C. L. The nitrogen legacy: Emerging evidence of nitrogen accumulation in anthropogenic landscapes. *Environ. Res. Lett.* **11**, 035014 (2016).

36. Lomstein, B. A., Langerhuus, A. T., D'Hondt, S., Jørgensen, B. B. & Spivack, A. J. Endospore abundance, microbial growth and necromass turnover in deep sub-seafloor sediment. *Nature* **484**, 101–104 (2012).

37. Fernandez, C. W., Langley, J. A., Chapman, S., McCormack, M. L. & Koide, R. T. The decomposition of ectomycorrhizal fungal necromass. *Soil Biol. Biochem.* **93**, 38–49 (2016).

38. Throckmorton, H. M., Bird, J. A., Dane, L., Firestone, M. K. & Horwath, W. R. The source of microbial C has little impact on soil organic matter stabilisation in forest ecosystems. *Ecol. Lett.* **15**, 1257–1265 (2012).

39. Buckeridge, K. M. et al. Sticky dead microbes: Rapid abiotic retention of microbial necromass in soil. *Soil Biol. Biochem.* **149**, 107929 (2020).

40. Jilling, A. et al. Minerals in the rhizosphere: Overlooked mediators of soil nitrogen availability to plants and microbes. *Biogeochemistry* **139**, 103–122 (2018).

41. Sokol, N. W., Sanderman, J. & Bradford, M. A. Pathways of mineral-associated soil organic matter formation: Integrating the role of plant carbon source, chemistry, and point of entry. *Glob. Chang. Biol.* **25**, 12–24 (2019).

42. Kuzyakov, Y. Priming effects: Interactions between living and dead organic matter. *Soil Biol. Biochem.* **42**, 1363–1371 (2010).

43. Manzoni, S., Jackson, R. B., Trofymow, J. A. & Porporato, A. The global stoichiometry of litter nitrogen mineralization. *Science*. **321**, 684–686 (2008).

44. Fernandez, C. W., Heckman, K., Kolka, R. & Kennedy, P. G. Melanin mitigates the accelerated decay of mycorrhizal necromass with peatland warming. *Ecol. Lett.* **22**, 498–505 (2019).

45. Certano, A. K., Fernandez, C. W., Heckman, K. A. & Kennedy, P. G. The afterlife effects of fungal morphology: Contrasting decomposition rates between diffuse and rhizomorphic necromass. *Soil Biol. Biochem.* **126**, 76–81 (2018).

46. Ma, L. et al. Assembly and development of the Pseudomonas aeruginosa biofilm matrix. *PLoS Pathog.* **5**, e1000354 (2009).

47. Parsons, L. L., Smith, M. S. & Murray, R. E. Soil denitrification dynamics: Spatial and temporal variations of enzyme activity, populations, and nitrogen gas loss. *Soil Sci. Soc. Am. J.* **55**, 90–95 (1991).

48. Kuzyakov, Y. & Blagodatskaya, E. Microbial hotspots and hot moments in soil: Concept & review. *Soil Biol. Biochem.* **83**, 184–199 (2015).

49. Bardgett, R. D., Lovell, R. D., Hobbs, P. J. & Jarvis, S. C. Seasonal changes in soil microbial communities along a fertility gradient of temperate grasslands. *Soil Biol. Biochem.* **31**, 1021–1030 (1999).

50. Hu, Y., Zheng, Q., Noll, L., Zhang, S. & Wanek, W. Direct measurement of the in situ decomposition of microbial-derived soil organic matter. *Soil Biol. Biochem.* **141**, 107660 (2020).

51. Blagodatskaya, E., Yuyukina, T., Blagodatsky, S. & Kuzyakov, Y. Turnover of soil organic matter and of microbial biomass under C3-C4 vegetation change: Consideration of 13 C fractionation and preferential substrate utilization. *Soil Biol. Biochem.* **43**, 159–166 (2011).

52. Chen, L. et al. Soil carbon persistence governed by plant input and mineral protection at regional and global scales. *Ecol. Lett.* **24**, 1018–1028 (2021).

53. Johnson, M. S. & Lehmann, J. Double-funneling of trees: Stemflow and root-induced preferential flow. *Ecoscience* **13**, 324–333 (2006).

54. Baggs, E. M. Soil microbial sources of nitrous oxide: Recent advances in knowledge, emerging challenges and future direction. *Curr. Opin. Environ. Sustain.* **3**, 321–327 (2011).

55. Moreau, D., Bardgett, R. D., Finlay, R. D., Jones, D. L. & Philippot, L. A plant perspective on nitrogen cycling in the rhizosphere. *Funct. Ecol.* **33**, 540–552 (2019).

56. Keiluweit, M. et al. Mineral protection of soil carbon counteracted by root exudates. *Nat. Clim. Chang.* **5**, 588–595 (2015).

57. Derrien, D. & Amelung, W. Computing the mean residence time of soil carbon fractions using stable isotopes: Impacts of the model framework. *Eur. J. Soil Sci.* **62**, 237–252 (2011).

58. Beidler, K. V. et al. Substrate quality drives fungal necromass decay and decomposer community structure under contrasting vegetation types. *J. Ecol.* **108**, 1845–1859 (2020).

59. Gunina, A., Dippold, M., Glaser, B. & Kuzyakov, Y. Turnover of microbial groups and cell components in soil: 13 C analysis of cellular biomarkers. *Biogeosciences* **14**, 271–283 (2017).

60. Wang, C. et al. Stabilization of microbial residues in soil organic matter after two years of decomposition. *Soil Biol. Biochem.* **141**, 107687 (2020).

61. Robertson, A. D. et al. Unifying soil organic matter formation and persistence frameworks: the MEMS model. *Biogeosci. Discuss.* 1–36 https://doi.org/10.5194/bg-2018-430 (2018).

62. R Core Team. R: A language and environment for statistical computing. (2020).

63. Fierer, N. & Schimel, J. P. A proposed mechanism for the pulse in carbon dioxide production commonly observed following the rapid rewetting of a dry soil. *Soil Sci. Soc. Am. J.* **67**, 798 (2003).

64. Maddison, A. L. et al. Predicting future biomass yield in Miscanthus using the carbohydrate metabolic profile as a biomarker. *GCB Bioenergy* **9**, 1264–1278 (2017).

65. Lopez-Sangil, L. & Rovira, P. Sequential chemical extractions of the mineral-associated soil organic matter: An integrated approach for the fractionation of organo-mineral complexes. *Soil Biol. Biochem.* **62**, 57–67 (2013).

66. Pinheiro, J., Bates, D., DebRoy, S. & Sarkar, D. nlme: Linear and nonlinear mixed effects models. *R package version* **3**, 1–144 (2020).

67. Wickham, H. ggplot2: Elegant Graphics for Data Analysis. (Springer-Verlag, 2016).

68. Buckeridge, K. M. kmbuckeridge/UGrass_NecromassCNstabilization: Necromass CN stabilization (v1.0). Zenodo. https://doi.org/10.5281/zenodo.5056539 (2021).

Acknowledgements

Author contributions
KB conceptualized the study, developed the experimental design, led the experimental research, sample analysis, data analysis and writing. KM contributed to the concepts and experimental design, experimental research and sample analysis, and manuscript revisions. NO contributed to the concepts, experimental design, and manuscript revisions. NMN contributed to the concepts, experimental design, sample analysis, and manuscript revisions. HG contributed to sample analysis and manuscript revisions. JW contributed to the concepts, experimental design, data analysis, and manuscript revisions.

Competing interests
The authors declare no competing interests.

Additional information
Supplementary information The online version contains supplementary material available at https://doi.org/10.1038/s43247-022-00439-0.

Correspondence and requests for materials should be addressed to Kate M. Buckeridge.

Peer review information *Communications Earth & Environment* and the authors thank the anonymous reviewers for their contribution to the peer review of this work. Primary Handling Editors: Clare Davis. Peer reviewer reports are available.

Reprints and permission information is available at http://www.nature.com/reprints

Publisher's note Springer Nature remains neutral with regard to jurisdictional claims in published maps and institutional affiliations.